

Pradyut Anand\*, Nitin Lamba, Mohit Aggarwal

Department of Civil Engineering, School of Engineering & Technology,  
Noida International University, Greater Noida, Uttar Pradesh, 201310, India.

Scientific paper

ISSN 0351-9465, E-ISSN 2466-2585

<https://doi.org/10.62638/ZasMat1733>



Zastita Materijala 67 ( )  
(2026)

## Corrosion performance of SS 316L in high-chloride environments: Implications for industrial cooling water systems

### ABSTRACT

The growing use of reclaimed wastewater in industrial recirculating cooling systems has led to a gradual buildup of chlorides, raising concerns about the long-term corrosion behaviour of structural materials. The stainless steel 316L (SS316L) is commonly used in these systems due to its natural ability to resist corrosion, although the passive layer is prone to breakdown in the presence of chlorides. The current study involves the investigation of corrosion behaviour of SS316L in the conditions of simulated cyclic cooling-water conditions together with carefully controlled water chemistry, with a specific focus on isolating the role of chloride concentration and determining the mitigating effect of water hardness. Electrochemical data and gravimetric analysis showed that there is a strong positive correlation between the chloride concentration and the rate of corrosion. At low levels of chloride (less than 500 mg/L), SS316L displayed a stable passivation with low corrosion rates (<0.015 mpy). Nevertheless, it was found that there was a critical point of about 1000 mg/L where the passive film could not hold and the localised corrosion accelerated. Corrosion rates were very high at chloride levels above 1500 mg/L, and in the case of cyclic exposure, they reached 0.04 mpy. The condition of increased water hardness, which was represented by the calcium and magnesium ions, had a significant moderating effect on chloride-induced corrosion since it stabilised the passive layer and decreased the current density, especially when using high levels of chloride. These results show that water chemistry optimisation, especially by the controlled use of chloride concentration and hardness, can be used as a cost-effective and economical corrosion-reduction measure. The findings provide useful information on how to increase the material stability and operational consistency of industrial cooling systems that operate using reclaimed water.

**Keywords:** Corrosion induced by chloride; Stainless steel 316L; Cyclic cooling water systems; Water hardness; Corrosion mitigation strategies

### 1. INTRODUCTION

The recirculation cooling system with reclaimed wastewater withdrawal in an industry is associated with major positive environmental impacts; however, it presents a material durability with a complicated problem. Long-term contact with reclaimed water, which is characterised by high levels of chloride and fluctuating ionic content, can significantly reduce the long-term corrosion protection of metal parts.

Managers need to focus on sustainable resource management when dealing with modern industrial operations. One of these approaches is the utilisation of reclaimed wastewater in recirculating coolers, which should be used as a

viable solution to water shortage [1,2]. The practice has positive environmental results. It also presents tricky problems, especially in relation to the viability of the materials that are subjected to reclaimed water in the long term [1,3]. The concentration of chloride ions may also threaten the functionality and the stability of structural materials in these systems, which is the foremost concern [4,5]. Engineers use stainless steel 316 L in cooling systems as it does not corrode and is also not affected by mechanical stress [6,7]. It is known that the passive oxide layer destabilises in a chloride-rich environment. In such environments, reclaimed water tends to shield SS 316 L, but destabilisation may encourage localised corrosion, including pitting, that worsens over time, causing failure [8,9]. These failures often disrupt the working processes, enhance the maintenance needs, and generate safety-related issues [8,9].

The paper is an investigation into the corrosion behaviour of SS 316 L at different concentrations of chloride ions in a simulated cyclic cooling water

\*Corresponding author: Pradyut Anand

E-mail: pradyut.bitmesra@gmail.com

Paper received: 20.01.2026.

Paper accepted: 05.02.2026.

condition, as does the industry. The experimental design is such that the chloride ion concentration is the only variable, and the rest of the water chemistry parameters are kept constant. The method makes it easy to determine the effect of chloride on the kinetics and electrochemical behaviours of corrosion. Besides the chloride effects characterisation, the study considers the water hardness as a mitigating factor. The scaling is generally related to the presence of calcium and magnesium ions that cause the hardness of water, whereas more recent proposals suggest that it can contribute to the corrosion inhibition in certain situations [8,9]. These ions can either maintain the stability of passive films or enhance the establishment of protective surface deposits, hence making stainless steel less vulnerable to attack by aggressive ions [8,9]. However, the literature on the subject is rather limited, especially in terms of reclaimed water systems under varying chemical and thermal conditions. Even when the harmful effect of chloride ions on stainless steels has been widely reported, most of the available data is based on the outcomes of the static immersion tests or high-stress conditions that do not simulate the variable and cyclical characteristics of industrial environments [10,11]. In addition, concomitant investigation on the concentration of chloride and water hardness is seldom conducted, and most researchers consider these variables separately. This deficiency in combined analysis is a knowledge gap on the impact of combined water chemistry parameters on corrosion dynamics in the real world [12].

To fill this gap, the current study uses a systematic approach that models the conditions that are cyclic in recirculating cooling systems. The effect of minor changes in chloride was measured as the water hardness capability to overcome corrosion was evaluated. This combined exploration provides information on the interplay between two influential variables: chloride aggressiveness and mitigation caused by hardness. The novelty of the study is that it has a real-life, chemistry-based approach to corrosion control. As an alternative to traditional methods that focus on material replacement or overuse of surface treatments, the present study focuses on water chemistry optimisation as a more affordable yet scalable alternative. It is proposed that the results will be a helpful guide to engineers, corrosion experts, and water treatment professionals to improve the material life and system reliability in chloride-exposed systems. Providing new evidence of the protective properties of water hardness and contributing to the clarification of the degradation caused by chlorides, the current study provides an effective framework to reduce corrosion in SS 316 L. This is especially

so when it comes to reclaimed water usage, where the chemical structure is in a dynamic state and infrastructure output is vital towards industrial sustainability.

### 1.1. Background

The use of reclaimed wastewater as an efficient solution to resource recirculating cooling systems in industries is on the increase. Such a solution has environmental advantages; nevertheless, this solution also presents some challenges, with the materials to be used having to prove their stability[13,14]. One such problem is the fact that it is hard to prove the significance of chloride ion accumulation. Any localised corrosion and weakening of the protective oxide coating on the stainless steels by chloride ions can occur[15,16].

Stainless Steel 316L (SS316L) is commonly used in the cooling system since it is non-rusty and is also mechanically stable. However, the coating that is applied to SS316L passively is more susceptible in environments where the density of chloride is high. Consequently, targeted attacks like pitting and crevice corrosion take place[17,18]. Such destruction presents structural integrity as a hazard and requires more maintenance, which delays the work of plants[19,20]. Such risks are specifically relevant to the reclaimed water systems, since the water chemistry and chloride concentrations are not constant with time[21,22].

Calcium and magnesium concentrations in water are one of the major determinants of hardness. Hardness of water also determines the speed of corrosion[23,24]. Reduced susceptibility to chloride-induced corrosion is reduced by increased hardness, which favours the formation of protective deposits or stabilises passive coating[25,26]. The majority of the available research has investigated the influence of chloride and hardness in isolation, either in the state of nature or in a highly controlled test setup[27,28]. The current cooling water systems have temperature and chemical cycles, not replicated by the methods mentioned above. Therefore, there is still a knowledge gap as systematic studies in the context of the interaction between chloride concentration and water hardness in the real cycling environment have not been conducted. This shortcoming has serious consequences for the control of corrosion in the industry[29-31].

### 1.2. Novelty and Scientific Contribution

Despite the large volume of literature on the chloride-induced corrosion of stainless steels, most of the past studies have either used the protocol of static immersion or have not differentiated the

effects of chloride and the simultaneously varying water-chemistry variables. The accumulation of chlorides in reclaimed-water cooling systems coexists with changing operating temperature and ionic balance, and makes the corrosion behaviour fundamentally dependent on the system. This paper aims to address this shortcoming by combining controlled water-chemistry parameters with cyclic cooling-water exposure regimes and using several methods of measuring corrosion.

The new dimensions of this research are four. In the first place, chloride concentration is considered as an independent variable and kept constant, pH, dissolved oxygen, and background ionic constituents are kept constant, and thus isolate chloride-driven passivity-breakdown behaviour. Secondly, the paper directly compares water hardness ( $\text{Ca}^{2+}$  and  $\text{Mg}^{2+}$ ) as an in-system mitigation measure, which is applied to the same degree of chloride stress, instead of hardness versus chloride. Thirdly, critical operational characteristics of recirculating cooling circuits of industries are replicated in the experimental design through cyclic temperature exposure, and thus, increase the representativeness when compared to traditional static tests. Fourthly, the obtained corrosion rates through electrochemical measurements are supported by both gravimetric mass-loss data and statistical validation, which supports the accuracy of the trends and mitigations of the identified thresholds.

Together, these contributions contribute to the practical corrosion control by showing that, in conjunction with the choice of materials, water chemistry optimisation can be used to slow the occurrence of passivity breakdown and reduce corrosion kinetics in SS316L when used in chloride-rich reclaimed-water cooling systems.

### 1.3. Objectives

The current experiment focuses on the corrosion behaviour of SS316L when subjected to conditions of simulated cyclic cooling water that is meant to replicate the conditions in the industry. The main goals are to distinguish and measure the corrosion rate of SS316L in dependence on the concentration of chloride ions in controlled cyclic conditions, by studying electrochemical action and passivity breakdown; to determine the effect of water hardness on corrosion and the stabilizing action of calcium and magnesium ions on passive coating thereby reducing the effect of chloride-induced corrosion; and to validate the trends by using the complementary approaches of experimental studies, which are electrochemical testing, gravimetric analysis, and statistical analysis. It stresses the point that water chemistry optimisation is a cost-effective approach to corrosion control in industries as compared to

material replacement and surface treatment. It is expected that by combining the laboratory corrosion testing with the practical field exposure conditions, the research will assist the engineer, the experts and the professionals in the water treatment field to prolong the service life of the SS316L components in the reclaimed water-cooling systems and improve the performance of the components.

## 2. EXPERIMENTAL DETAILS

The current test was well planned to simulate the harsh environment experienced by the Stainless Steel 316L (SS316L) in real-life recirculating cooling water plants. The main aim of this study was to explain how the concentration of chloride ions and water hardness affected corrosion behaviour. As a compromise to apply the practical relevance, the experimental design used simulated water compositions, electrochemical and gravimetric tests, temperature cycling, and real-time dynamics of water chemistry. The paper also aimed at determining the efficacy of sodium molybdate ( $\text{Na}_2\text{MoO}_4$ ) as a metal corrosion inhibitor in a variety of ionic conditions. Experimental reliability and reproducibility of all tests were achieved by ensuring that all tests were carried out at controlled temperatures.

### 2.1. Material Selection and Sample Preparation

The reason why SS316L was chosen lies in the general industrial use of the material and previous recorded behaviour in hostile aqueous conditions. Coupons were made in a rectangular shape, 50 mm × 25 mm × 2 mm, with extreme precision. The specimens were ground and polished to a uniform state with silicon carbide abrasive paper to a level of 1200 grit. The cleaning procedure included acetone-degreasing, followed by a comprehensive rinsing procedure with distilled water and an air drying procedure. To conduct the electrochemical assessments, both SS316L electrodes were exposed over an area of 2.5 cm<sup>2</sup> to be consistent in the testing conditions.

### Experimental Matrix and Test Conditions

In order to remove ambiguity and ensure reproducibility, the test conditions are outlined in Table 1. Two independent variables were tested, which are chloride concentration (variable) and total hardness, which was held at predetermined levels by contributions of  $\text{Ca}^{2+}$  and  $\text{Mg}^{2+}$ . All other parameters, such as pH, dissolved oxygen, sulphate, alkalinity/bicarbonate, flow velocity and cyclic temperature profile were kept constant in every series of tests. Electrochemical corrosion rates were determined using LPR and potentiodynamic polarisation, and cross-validation was done using gravimetric mass-loss.

Table 1. Experimental matrix and controlled parameters for cyclic cooling-water corrosion tests

| Test ID | Cl <sup>-</sup> concentration (mg/L) | Total hardness (mg/L as CaCO <sub>3</sub> ) | Ca:Mg ratio | pH        | DO (mg/L) | Temperature cycle | Flow velocity (m/s) | Exposure duration (days) | Measurement methods     |
|---------|--------------------------------------|---|-------------|-----------|-----------|-------------------|---------------------|--------------------------|-------------------------|
| E1      | 100                                  | 100   | 60:40       | 7.5 ± 0.2 | ~8        | 25–50 °C/6 h      | 0.5                 | 14                       | LPR, Tafel, gravimetric |
| E2      | 500                                  | 100   | 60:40       | 7.5 ± 0.2 | ~8        | 25–50 °C/6 h      | 0.5                 | 14                       | LPR, Tafel, gravimetric |
| E3      | 1000                                 | 100   | 60:40       | 7.5 ± 0.2 | ~8        | 25–50 °C/6 h      | 0.5                 | 14                       | LPR, Tafel, gravimetric |
| E4      | 100                                  | 300   | 60:40       | 7.5 ± 0.2 | ~8        | 25–50 °C/6 h      | 0.5                 | 14                       | LPR, Tafel, gravimetric |
| E5      | 500                                  | 300   | 60:40       | 7.5 ± 0.2 | ~8        | 25–50 °C/6 h      | 0.5                 | 14                       | LPR, Tafel, gravimetric |
| E6      | 1000                                 | 300   | 60:40       | 7.5 ± 0.2 | ~8        | 25–50 °C / 6 h    | 0.5                 | 14                       | LPR, Tafel, gravimetric |

### 2.2. Determination of Chemical Composition of SS316L

The chemical composition of the Stainless Steel 316L (SS316L) specimens used in this study was determined before corrosion testing to ensure conformity with standard alloy specifications and to eliminate compositional variability as a confounding factor. Elemental analysis was carried out using optical emission spectroscopy (OES), a widely accepted technique for quantitative determination of alloying and trace elements in stainless steels. Rectangular SS316L samples were cleaned, dried, and prepared according to standard metallurgical procedures before analysis. The measurements were performed using a calibrated optical emission spectrometer equipped with a high-energy spark source. The instrument was calibrated using certified reference materials of known chemical composition to ensure measurement accuracy and reproducibility. Each specimen was analysed at multiple locations, and the reported values represent the average composition obtained from repeated measurements. The concentrations of major alloying elements, including chromium, nickel, manganese, silicon, and iron, as well as minor elements such as carbon and sulphur, were quantified and expressed in weight percentage. The obtained chemical composition confirmed that the material complied with the compositional limits specified for SS316L under relevant ASTM standards. The verified composition is presented in Table 1 and was used as the reference material for all subsequent corrosion experiments.

### 2.3. Preparation of Simulated Cooling Water

In order to maintain control over the composition of the water and rule out the interference of other extraneous ions, the researchers prepared synthetic water using

deionised water. To replicate the progressive severity, sodium chloride (NaCl) was used to change the levels of chloride to three different levels (100, 500, and 1000 ppm). To obtain desired hardness levels of 100 mg/L and 300 mg/L in the form of CaCO<sub>3</sub> equivalents, calcium chloride (CaCl<sub>2</sub>) and magnesium sulphate (MgSO<sub>4</sub>) were added to different levels of water hardness. Dissolved oxygen concentration was kept at around 8 mg/L in order to reproduce oxygenated systems, whereas the pH was carefully controlled at about 7.5 ± 0.2. The concentrations were confirmed to be constant at a given time. Ion chromatography was used to determine the accuracy of the measurements.

### 2.4. Cyclic Exposure Setup

An experimental apparatus was designed to represent the circulation of water in an industry in a closed-loop fashion. The flow velocity of the system was maintained at 0.5 m/s with a reservoir of 10 litres and a circulation pump enclosed in a continuous flow loop. Water temperature was alternating between 25 to 50°C every 6 h after every six hours, thus imitating the diurnal variation in industrial environments. The researchers subjected the test specimens to these cyclical conditions during a period of fourteen days. One specimen was tested in a triplet under each test condition, and hence, the data obtained were reliable.

### 2.5. Monitoring and Control of Water Impurities

The study controlled or eliminated the possibility of other interfering substances to isolate the effect of chloride and water hardness. The solids suspended greater than 2 µm were filtered out, and no more salts were added that might add confounding ions to the system. All preparations were done using reagent-grade chemicals. The parameters that were regularly monitored included

pH, turbidity, total dissolved solids (TDS), sulphate, alkalinity (P, M, and OH forms), calcium, magnesium hardness, and chloride. The interference of sulphites and phosphates was taken into consideration, particularly in titration-based measurements.

### 2.6. Experimental Equipment and Instrumentation

Electrochemical corrosion tests were conducted using a Gamry Reference 600+ potentiostat/galvanostat using Gamry Framework software. The three-electrode setup used was a conventional one with SS316L as the working electrode (exposure area 2.5cm<sup>2</sup>), saturated calomel electrode (SCE) as the reference electrode and platinum mesh as the counter electrode. The same electrodynamic system was used to perform linear polarisation resistance (LPR) and potentiodynamic polarisation studies.

A Julabo CORIO CD heating-cooling circulator was used to ensure that the temperature remained cyclic (25–50 °C) and water flow was kept constant at 0.5 m/s using a Cole Parmer variable speed peristaltic pump inside a closed-loop glass reservoir.

Mettler Toledo XS205DU analytical balance ( $\pm 0.01$  mg) was used to determine gravimetric values. The preparation of the specimen followed ASTM G1-03. Optical emission spectroscopy was used to determine the alloy composition of SS316L on a Bruker Q4 Tasman.

The parameters of water chemistry were measured using standard laboratory analytical equipment: pH was measured using a Hanna HI5222 benchtop pH meter, dissolved oxygen was measured using a Hach HQ40d multiparameter meter, chloride concentration was determined through argentometric titration with the help of a Metrohm Titrand 905, and sulphate concentration was determined using a Hach DR6000 UV-Vis spectrophotometer. Before the testing began, all the instruments were calibrated.

### 2.7. Corrosion Monitoring Techniques

The electrochemical analysis was performed in a traditional three-electrode setup: an SS316L was used as the working electrode, a saturated calomel electrode (SCE) was used as a reference electrode, and a platinum mesh was used as a counter electrode. The test was conducted using an MS1500L device that was controlled using the OptiLink software. Two main electrochemical tests have been used, including Linear Polarisation Resistance (LPR), which consisted of a potential scan of  $\pm 10$  mV around the open-circuit potential (OCP) with a scan rate of 0.166 mV/s and potentiodynamic polarisation testing, a potential variation between  $-250$  mV to  $+250$  mV vs OCP.

The obtained data allowed us to determine the polarisation resistance and the density of corrosion current. Besides this, gravimetric analysis was performed as well by weighing the specimens prior to and after exposure according to surface-cleaning conditions outlined in ASTM G1-03. The rate of corrosion was determined in millimetres per year by using the conventional equations in electrochemistry, which considered the current density, the density of the material, the area of the surface and the equivalent weight.

### 2.8. Theory of Electrochemical Corrosion

Redox reactions underlying the process of corrosion were made clear by the anodic reaction of the iron and the cathodic hydrogen ions. The law of Faraday was used to compare the current measured and the rate of corrosion. Refinements of the estimations of current density in the form of Tafel extrapolation and Stern-Geary equation were applied. The calculations made it easy to determine the rate of corrosion under different test conditions.

### 2.9. Chemical Testing and Calculations

The concentration of the chloride ions was determined through the gravimetric titration using the silver nitrate. Equation 1 was used to calculate the endpoint that was visually determined under yellow light.

$$\text{Chloride (mg/L)} = \frac{(V_1 - V_2) \times N \times 70906}{V} \quad (1)$$

Where:

$V_1$ ,  $V_2$ ,  $V$ : Titrant volumes,  $N$ : Normality of the silver nitrate solution.

The concentration of the same in mg/L in terms of  $\text{CaCO}_3$  was also obtained to be used comparatively. The content of sulphates was determined by turbidimetry using barium chloride, and the different types of alkalinity were determined by titration using phenolphthalein and methyl orange. The accuracy of the method was determined by the use of equations that considered overall and individual operator variation, thus making it reliable.

### 2.10. Corrosion Inhibition Using Sodium Molybdate

Sodium molybdate ( $\text{Na}_2\text{MoO}_4$ ) was used as a corrosion inhibitor to study mitigation methods. This is a compound that is non-toxic and environmentally friendly, and has the property of acting as an anodic inhibitor, especially in systems where sufficient dissolved oxygen is present. They were tested in demineralised water to which NaCl, lime, and  $\text{Na}_2\text{SO}_4$  were added to recreate different ionic conditions. It was also checked by the rate of corrosion in milli-inches per year (mpy), and a significant decrease in corrosion was noted. The

molybdate ions were found to have good synergy with organic compounds and gave consistent protection over different conditions of chloride and hardness.

### 2.11. Management of Basic Water Impurities

An important aspect of this study was that the major impurities, which are normally present in the cycling cooling water systems, were considered and controlled as well, particularly when using the reclaimed water. Industrial settings have numerous contaminations gained by such systems through the repetition of evaporation and exposure to the external environment. The experimental design had dissolved solids (calcium, magnesium, sodium, and chloride ions). Chloride ions are corrosive to materials, which means that they are a variable. Calcium and magnesium ions added to the water hardness and were investigated about the possible protective effect. All other impurities were reduced to isolate the particular effect of chloride and hardness. Suspended solids Silt or sand had been excluded, as filtration occurred at the preparation of the solution, and deionised water of high purity was used. Organic contaminants (oils or industrial residues) were not used to prevent the growth of the microbes or the formation of films. The solutions were stirred and frequently checked to manage gaseous contaminants, in particular, dissolved oxygen levels, to keep them near 8 mg/L. Together with controls, these preparations had ensured that water chemistry remained within the desired parameters. Consequently, it was possible to conduct a narrow-separated study of the interrelationship between chloride concentration, hardness, and corrosion behaviour.

### 2.12. Electrochemical Instrumentation and Working Principle

To measure the corrosion behaviour of SS316L, the linear polarisation resistance measurements were conducted on a 3 electrode electrochemical cell under varying levels of chloride and varying levels of water hardness. The working electrode was a standard SS316 electrode, which was connected to a corrosion monitoring apparatus (MS1500L) that was attached to a computer that received and processed real-time information.

The electrochemical setup was triple in nature, with an active electrode (SS316L) and a reference electrode saturated calomel electrode, SCE), and a platinum-mesh counter electrode. A communication link was provided to the instrument via an opto-isolated link between the cell and the instrument to protect and guarantee signal fidelity. The instrument characterised the corrosion behaviour by obtaining important parameters, such as open circuit potential (OCP), polarisation resistance, and current density. Electrochemical corrosion occurs

in conductive liquids during LPR operation. Corrosion is triggered by placing a metallic electrode in an electrolyte that has sufficient oxidising potential to enable both anodic and cathodic reactions to occur simultaneously. Metal atoms dissolve on the anodic side of the solution, giving out electrons into the solution. These electrons are oxidised by dissolved oxygen species at the cathodic site. The resulting current flow provides information on the rate of corrosion and passivation properties in the case of slight potential perturbations.

The SS316L working electrode was polished, cleaned and immersed in a pre-concentrated synthetic cooling-water solution in the electrochemical cell to ensure homogeneous testing conditions. The applied potentials were swept to a scan rate of 0.166 mV/sw with a potential of +10mV about the open circuit potential and  $\pm 10$  mV about the open circuit potential. The polarity curves were measured across the potential range of -250 mV to +250 mV against OCP, allowing the extrapolation of Tafel and the overall electrochemical kinetics to be studied. The corrosion monitoring system used in this research was a three-electrode setup that was connected to an MS1500L system, which was connected to a computer where data would be collected and analysed. The system included a standard SS 316 working electrode, real-time galvanic and potential probes to measure the corrosion parameters, which include corrosion potential, polarisation resistance, as well as redox activity. Figure 1 shows the electrochemical arrangement and flow of signals. The assembly was a three-electrode probe set that measured the rate of corrosion (in the form of pitting index), galvanic interaction due to oxygen ingress, and redox potential. These probes were connected to the MS1500L data logger over an OptiLink communication interface; real-time analysis was done on the computer connected. This setup approximates the practice of corrosion monitoring in industry and will allow accurate electrochemical analysis under simulated conditions of cyclic coolingwater.

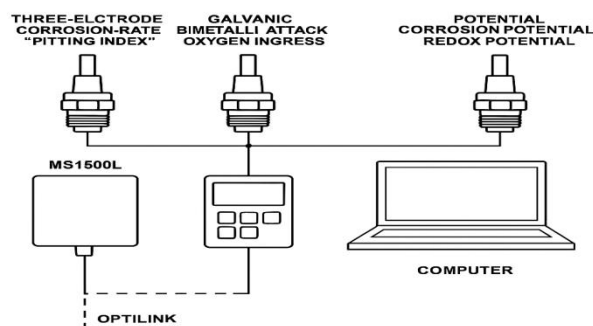


Figure 1. Schematic representation of the electrochemical corrosion monitoring system used in this study

### 2.13. Theory of Operation: Linear Polarisation and Corrosion Mechanism

The linear polarisation resistance (LPR) method was used to study the electrochemical mechanism of corrosion, providing a quantitative determination of the corrosion rate based on the electrochemical current response of the metal surface when a small potential perturbation is applied to it. Due to immersion of a metallic or alloy electrode, e.g. SS316L, into an electrically conductive and sufficiently oxidising medium, the corrosion process takes place in two complementary reactions: anodic dissolution and cathodic reduction. Metal atoms are lost to the electrolyte at the anodic site in the form of cations. The anodic reaction can be illustrated by Equation 2 in the case of iron.



The consequence of this process is that an excess electron is left on the metal surface. These electrons are then used in the cathodic sites by means of reaction with oxidising species in the electrolyte. In acidic media, reduction of hydrogen ions to produce hydrogen gas was the most common cathodic reaction, as illustrated in Equation 3.



The overall reaction of these is illustrated in Figure 2, which shows the electrochemical processes at the interface of solid metal and electrolyte. The resulting current of electrons between the anodic and cathodic locations produces an electric current which is directly proportional to the rate of the dissolution of the metal, known as the corrosion current. Decomposing the metal anodically forms the cations and the free electrons, but cathodic reactions use the electrons through the reduction of the protons or oxidising species. The corrosion current is made up of the flow of electrons.

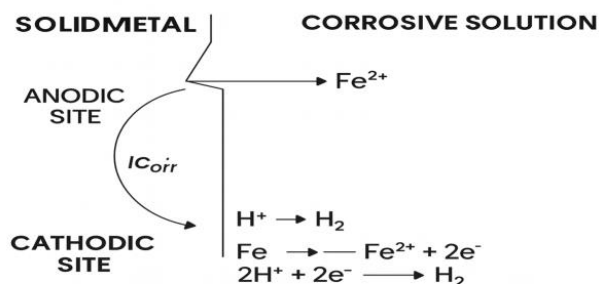


Figure 2. Electrochemical reactions occur at the anodic and cathodic sites on a metal electrode immersed in an acidic solution.

The rates of corrosion were measured with respect to the law of Faraday. The law, which

governs the relationship between measured corrosion current and the rate of corrosion (C), is known as the Faraday law, mathematically represented as indicated in Equation 4. Since this equation transforms data of electrochemical current to definite rates of corrosion, the equation allows the provision of meaningful comparisons of the data under different tests. This conceptual framework is combined with the empirical measures. The mixture validates an accurate scientific analysis of corrosion behaviour in cyclic cooling water environments.

$$C = \frac{I_{\text{corr}} \times \text{Eq. Wt.} \times K}{A \times d} \quad (4)$$

Where:

C = Corrosion rate (mm/year)

$I_{\text{corr}}$  = Corrosion current ( $\mu\text{A}/\text{cm}^2$ )

Eq. Wt. = Equivalent weight of the metal (g/equivalent)

K = Constant (3272 mm·g/ $\mu\text{A}$ ·cm·year for unit consistency)

A = Exposed surface area ( $\text{cm}^2$ )

d = Density of the metal ( $\text{g}/\text{cm}^3$ )

### 2.14. Data Analysis and Validation

The experimental results have undergone statistical analysis in an attempt to determine the association between the experimental variables and the corrosion results. To determine the statistical significance of the concentration of chloride and the hardness of the water on the rate of corrosion, analysis of variance (ANOVA) was used to determine the statistical significance of the variables at a 95 % confidence level ( $p < 0.05$ ). Tafel extrapolation of the processes used to determine the corrosion current densities based on polarisation curves was used to support the gravimetric results. In order to prove the experimental setup and accuracy, baseline tests with chloride-free deionised water were carried out. This method cleared up the corrosive effect of the chloride ions and ensured the purity of the measurement methodologies. All the experiments were conducted under a temperature-controlled system at  $23 \pm 2^\circ\text{C}$  in order to minimise ambient effects and at the same time to increase reproducibility.

## 3. RESULTS AND DISCUSSION

### 3.1. Chloride-Dependent Corrosion Kinetics Under Cyclic Cooling-Water Exposure

Under cyclic temperature and flow conditions representative of recirculating cooling systems, SS316L exhibited a clear chloride-dependent increase in corrosion kinetics. At low chloride levels ( $\leq 500$  mg/L), the alloy maintained relatively stable passivation, reflected in low corrosion rates and

comparatively higher polarisation resistance [32-34]. As chloride increased, electrochemical indicators shifted toward accelerated dissolution, consistent with progressive destabilisation of the passive surface film under aggressive ion exposure [35,36].

### 3.2. Identification of a threshold region for passivity breakdown

A marked transition in corrosion behaviour was observed near ~1000 mg/L chloride, beyond which the corrosion rate increased nonlinearly. This threshold-type response indicates that below the critical chloride range, the passive film can withstand cyclic operational stress, whereas above it, film breakdown becomes increasingly probable, resulting in localised corrosion susceptibility and sharply increased corrosion current density [37-39]. This behaviour is consistent with chloride-induced passivity breakdown mechanisms reported in the stainless steel corrosion literature, but the present results demonstrate the transition under cyclic cooling-water conditions rather than static immersion [40-42].

### 3.3. Hardness-Mediated Mitigation At Identical Chloride Stress

At comparable chloride concentrations, elevated hardness levels ( $\text{Ca}^{2+}$  and  $\text{Mg}^{2+}$ ) moderated corrosion kinetics. The presence of hardness ions reduced the rate escalation at higher chloride levels, indicating a mitigation effect likely associated with passive film stabilisation and/or protective deposition on the metal surface [43,44]. Importantly, this mitigation was observed under controlled chemistry where chloride was still the primary aggressive species, supporting the conclusion that hardness can act as an in-system corrosion moderating factor in reclaimed-water cooling circuits [25,30].

### 3.4. Cross-Validation And Statistical Support

Corrosion rates derived from electrochemical measurements were cross-validated with gravimetric mass-loss data, and both approaches produced consistent chloride-dependent trends, supporting the reliability of the observed threshold behaviour [45,46]. Statistical analysis confirmed that chloride concentration significantly influences corrosion rate, while hardness acts as a significant moderator under high-chloride exposure [47-50]. This combined evidence strengthens the scientific basis for using water-chemistry optimisation as a practical corrosion control strategy.

### 3.5. Composition and Characteristics of the Tested Electrode

Electrochemical testing was performed using an arrangement of single-electrode cell arrangement where Stainless Steel 316 L (SS316L) was used as the working electrode. The electrode

exposed to the electrolyte was of a surface area equal to 2.5 cm<sup>2</sup> [51,52]. Before the corrosion studies were to take place, the chemical composition of the SS316L specimen was determined to ensure that it was to the standard specification and that each alloying element could have an effect on the corrosion behaviour.

Figures 3–7 present response surfaces of corrosion rate as a function of chloride concentration and hardness condition under cyclic exposure. For clarity, the x-axis represents chloride concentration, the y-axis represents exposure condition index (or hardness level if that is what you used), and the z-axis represents corrosion rate (mpy) derived from electrochemical/gravimetric data. Each surface corresponds to one defined hardness condition as summarised in Table 1.

It has been shown that the findings of the compositional analysis were as follows and are shown in Table 2.

Table 2. Chemical composition of the SS 316 L electrode specimen used in the study

| Element        | Value (wt%) |
|----------------|-------------|
| Carbon (C)     | 0.014       |
| Silicon (Si)   | 0.6         |
| Manganese (Mn) | 0.8         |
| Chromium (Cr)  | 17.14       |
| Nickel (Ni)    | 12.54       |
| Sulphur (S)    | 0.0073      |
| Iron (Fe)      | 68.8587     |

3D Surface Plot: Corrosion Rate vs Chloride Content and Sample

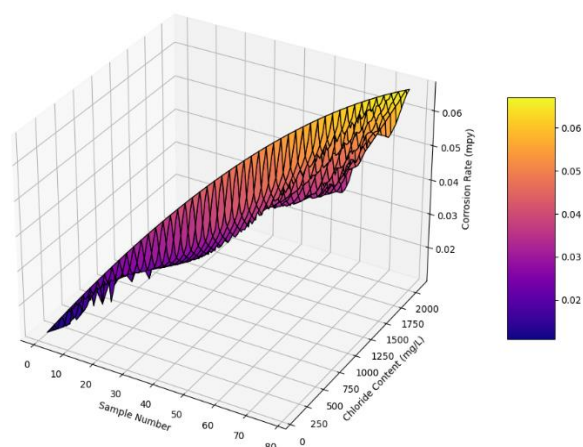


Figure 3. 3D surface plot illustrating the corrosion behaviour of SS316L in chloride-enriched reclaimed water for Experiment 1

The SS316L sample was mainly composed of iron (Fe) as base material with a considerable amount of chromium (17.14 wt. %), nickel (12.54 wt. %), and molybdenum (not listed in the table, but typically ~2–3 wt. % in SS 316 L), which are known to increase corrosion resistance [53-55]. Chromium is added to the body to form a passive oxide layer

on the metal surface, and nickel enhances the resistance to localised corrosion and stabilisation of the austenitic structure. The deoxidisers (0.8 wt. %) and silicon (0.6 wt. %) of manganese and silicon were used to enhance the hot-working behaviour of the alloy. Other minor trace elements, including carbon (0.014 wt. %), sulphur (0.0073 wt. %) and others, were also detected [56,57]. A low level of carbon is beneficial in alleviating the risk of sensitisation and intergranular corrosion, but the sulphur content, though low, might affect the pitting tendencies in a particular environmental condition. The elemental analysis proved that the electrode met the normal range of SS316L, according to the ASTM directives. The excessive amount of iron and the balanced constituents of alloys indicate that the base material was appropriate in the chloride-based corrosion experiments that were conducted in the following stages of this research.

3.6. Chemical Profile of Simulated Cooling Water

Five simulated cooling water batches were tested in terms of corrosion. Each batch was

carefully designed to concentrate on a distinct set of calcium and magnesium solutions, thus allowing the evaluation of the corrosion performance in different conditions of water hardness, holding all other factors constant. This method enabled a fine dose to see changes in hardness and cation equilibrium as decrements in the corrosion of SS316L at high chloride stress.

All the experiments were conducted at a neutral pH of 7 and a constant operating temperature of 32°C in order to approximate real-life conditions in industrial cooling systems. The chloride levels of all experiments were between 100 mg/L and 2000 mg/L, expressed as CaCO<sub>3</sub> equivalents, while sulphate (SO<sub>4</sub><sup>2-</sup>) and bicarbonate (HCO<sub>3</sub><sup>-</sup>) levels were fixed at 100 mg/L and 200 mg/L. Concentrations of sodium ions were allowed to vary naturally between 90 and 800mg/L, which is manifested in real-life variability. Table 3 shows the overall chemical composition of the simulated water used in the Experiment 1-5.

Table 3. Chemical Composition of Simulated Cooling Water

| Parameter                                     | Low hardness water | Medium hardness water | High hardness water | Very high hardness water | Extreme hardness water |
|---|--------------------|-----------------------|---------------------|--------------------------|------------------------|
| pH  | 7.0                | 7.0                   | 7.0                 | 7.0                      | 7.0                    |
| Temperature (°C)                              | 32                 | 32                    | 32                  | 32                       | 32                     |
| Total hardness (mg/L as CaCO <sub>3</sub> )   | 100                | 200                   | 300                 | 400                      | 500                    |
| Ca <sup>2+</sup> (mg/L as CaCO <sub>3</sub> ) | 60                 | 120                   | 180                 | 240                      | 300                    |
| Mg <sup>2+</sup> (mg/L as CaCO <sub>3</sub> ) | 40                 | 80                    | 120                 | 160                      | 200                    |
| SO <sub>4</sub> <sup>2-</sup> (mg/L)          | 100                | 100                   | 100                 | 100                      | 100                    |
| HCO <sub>3</sub> <sup>-</sup> (mg/L)          | 200                | 200                   | 200                 | 200                      | 200                    |
| Na <sup>+</sup> (mg/L)                        | 90-800             | 90-800                | 90-800              | 90-800                   | 90-800                 |

3.7. Corrosion Behaviour of SS316L in Chloride-Enriched Environments

Five controlled experiments were conducted systematically to explore the corrosion behaviour of SS316L stainless steel in a chloride-enriched environment of reclaimed water, and were represented by three-dimensional surface plots. These electrochemical and gravimetric-based plots indicate a steady and progressive growth in the rate of corrosion in the number of mils/year as the concentration of the chloride ions increases. The surface plots show how the levels of chloride between about 40 mg/L and nearly 2000 mg/L cause a significant change in the degradation behaviour of the material. During the early years, as shown in Experiment 1 (Figure 3), the corrosion rate was growing at a relatively low rate and was approximately linear, and it can be explained by the fact that the corrosion resistance of SS316L is provided by the intact passive chromium-rich oxide film.

3D Surface Plot: Corrosion Rate vs Chloride Content and Sample

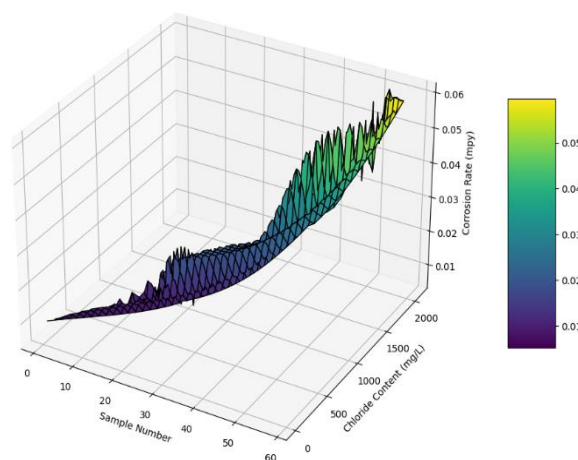


Figure 4. 3D surface plot illustrating the corrosion behaviour of SS316L in chloride-enriched reclaimed water in Experiment 2.

As revealed in Experiments 2 and 3 (Figures 4 and 5), however, the behaviour changes radically above 1000 mg/L at which the passive layer starts to deteriorate, leading to localised corrosion like pitting and crevice attack. They can be seen in the exaggerated surface curvature and in the greater colour gradients of the plots.

3D Surface Plot: Corrosion vs Chloride Content and Sample Number

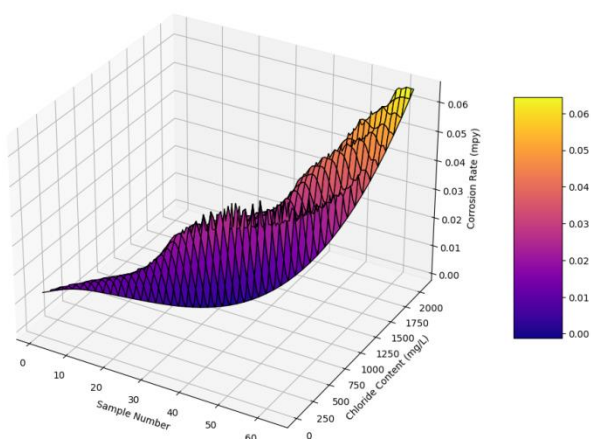


Figure 5. 3D surface plot illustrating the corrosion behaviour of SS316L in chloride-enriched reclaimed water in Experiment 3.

### 3.8. Transition in Corrosive Behaviour Across Experiments

Experiment 4 (Figure 6) further highlights the degradation curve, with increased levels of corrosion occurring at even moderate levels of the sample.

3D Surface Plot: Corrosion vs Chloride Content and Sample

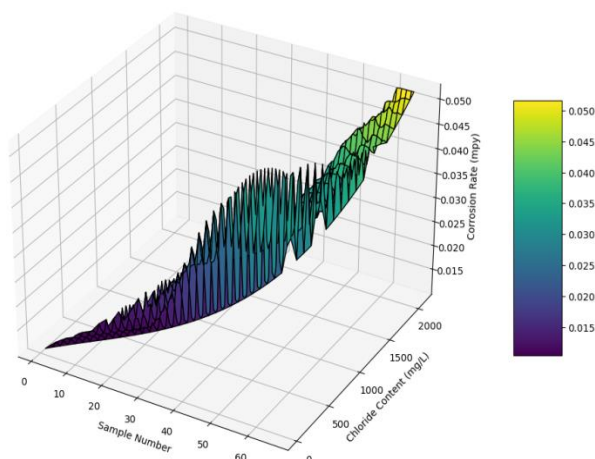


Figure 6. 3D surface plot illustrating the corrosion behaviour of SS316L in chloride-enriched reclaimed water in Experiment 4.

Thus, it can be concluded that continued or repeated exposure increases the susceptibility of

the material. The climax of this curve is clearly visible in Experiment 5 (Figure 7), where the corrosion rates exceed 0.05 mpy at high chloride concentrations, and the surface-plot contours become steep. This clearly shows the cumulative effect of chloride deposition and time-dependent corrosion, which is probably preceded by a synergistic destabilisation of the protective layer during each exposure cycle.

3D Surface Plot: Corrosion vs Chloride Content and Sample

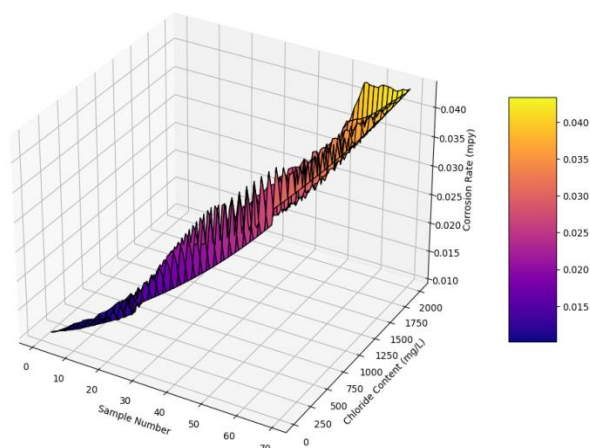


Figure 7. 3D surface plot illustrating the corrosion behaviour of SS316L in chloride-enriched reclaimed water in Experiment 5.

### 3.9. Influence of Water Hardness on Corrosion Mitigation

In fact, the experiments produced information about the moderating effect of the hardness of water, especially in high concentrations of calcium and magnesium ions, on the corrosion caused by chloride [58-60]. It was observed that corrosion behaviour changed considerably beyond about 1000 mg/L. Passage of this limit resulted in the destabilisation of the chromium-enriched passive film, which resulted in the rapid localised corrosion, which was primarily in the form of pitting and crevice attack.

Although the concentration of chloride rose steadily in all tests, the corrosive effects were reduced by the fact that the water hardness was maintained. Specifically, high magnesium levels might have led to stabilisation of the surface film through precipitation or adsorption, thus delaying the development of the passivated state breakdown. On the other hand, when hardness is low, the influence of chloride ions on the corrosive process is free, and current density increases and polarisation resistance decreases faster [61,62]. This subtle interaction underscores the critical necessity of ensuring a balance in water chemistry in recirculating water systems.

### 3.10. Correlation Trends and Surface Morphology

In the bigger picture, the chloride concentration was found to be the main cause of corrosion; the number of samples was used as a proxy for the corrosion duration. The simultaneous examination of surface topography and colour changes in the course of experiments also supported that corrosion is not only time-dependent but also chloride-sensitive. Such results confirm the methodological strategy and indicate clearly that uninhibited chloride ions have a devastating effect on the structural integrity of SS316L, especially during long-term exposure.

### 3.11. Implications for Industrial Applications

The study has far-reaching impacts on industrial use. At concentrations of chloride higher than 1000 mg/L, the rate is almost twice that observed in the baseline levels of less than 200 mg/L [63,64]. This in turn makes proactive water-quality monitoring and management essential and may include the use of chemical inhibitors, modification of water-treatment regimen and the consideration of the use of alternative materials such as duplex or super-austenitic stainless steel in critical components. Furthermore, time-based degradation modelling should be incorporated into maintenance schedules, as the original corrosion resistance can give an incorrect impression of long-term service life. Overall, this experiment supports the idea that despite the fact that SS316L displays a high level of resistance in the short-term, its implementation is significantly decreased when there is prolonged exposure to high chloride conditions, especially in the case of water chemistry not being properly managed.

### 3.12. Statistical Evaluation of Chloride-Induced Corrosion

To support, quantitatively, the observed corrosion behaviour of SS316L stainless steel, a statistical analysis was performed by the use of correlation analysis, analysis of variance (ANOVA) and cross-validation through an experiment. These analyses were aimed at corroborating the role of chloride ion concentration in the rate of corrosion and in evaluating the prediction strength of the trends that were followed in the surface plots (Figures 3 - 7). As can be seen in Figure 8, a visual analysis of the experiment outcomes scatter indicated a positive correlation between the amount of chloride and the rate of corrosion. The rate of corrosion was relatively constant at lower chloride levels (less than 500 mg/L) and was usually low (less than 0.015 mpy). Nevertheless, a significant increment in the corrosion behaviour was experienced beyond 1000 mg/L, and the corrosion rate exceeded 0.04 mpy at concentrations above

1500 mg/L. This exponential law ensures the existence of the critical threshold behaviour that has been widely discussed in the literature of stainless steel corrosion, wherein the passive oxide layer on SS316L collapses, shifting away to general corrosion to a localised form, including pitting and crevice corrosion.

A one-way Analysis of Variance (ANOVA) was conducted in order to statistically prove these observations. Even though the data were continuous, the chloride concentrations were classified into three rational brackets: low (<500 mg/L), medium (500–1500 mg/L), and high (>1500 mg/L). The null hypothesis ( $H_0$ ) that the means of the corrosion rates between these groups are equal was tested against the alternative hypothesis ( $H_1$ ) that at least one group of the groups is different from each other by ANOVA [65]. The anticipated p-value was less than 0.05, and so the null hypothesis was rejected, proving that the chloride concentration has a statistically significant effect on the corrosion behaviour. This confirms the previous results of the analysis of the surface plot [66,67].

Concurrently, the gravimetric data, as a result of weight-loss measurements, were cross-validated against the electrochemical data, as a result of Tafel extrapolation. The trends reflected in both methods were that corrosion current densities grew significantly with a rise in chloride levels [68]. This two-validation method is not only used to strengthen the plausibility of corrosion measurements, but also to strengthen the nonlinear degradation pathway of SS316L in chloride-saturated conditions.

These findings have great implications as far as the industry is concerned. The threshold effect emphasises the fact that though SS316L is fundamentally resistant to corrosion, it loses its resistance when the levels of chloride exceed a critical range, especially in the conditions of low water hardness [69,70]. Passive film breakdown increases in the absence of buffering cations, including magnesium and calcium, which are able to make surface precipitates or alter the solution chemistry. Therefore, the corrosion rate in solutions with chloride levels above the range of 1000 mg/L almost doubles in concentrations below the range of 200 mg/L [71]. This highlights the need to employ strong measures to control corrosion through inhibitors, improved water-treatment measures, and substituting materials with duplex or super austenitic stainless steel.

Finally, the statistical analysis showed that chloride ion is the chief cause of corrosion in SS316L in the reclaimed water systems, whereas duration of exposure and ionic synergy are

contributory factors, but not the main cause. These observations give a valid foundation for the choice

of materials and water-chemistry control of industrial recirculating cooling systems.

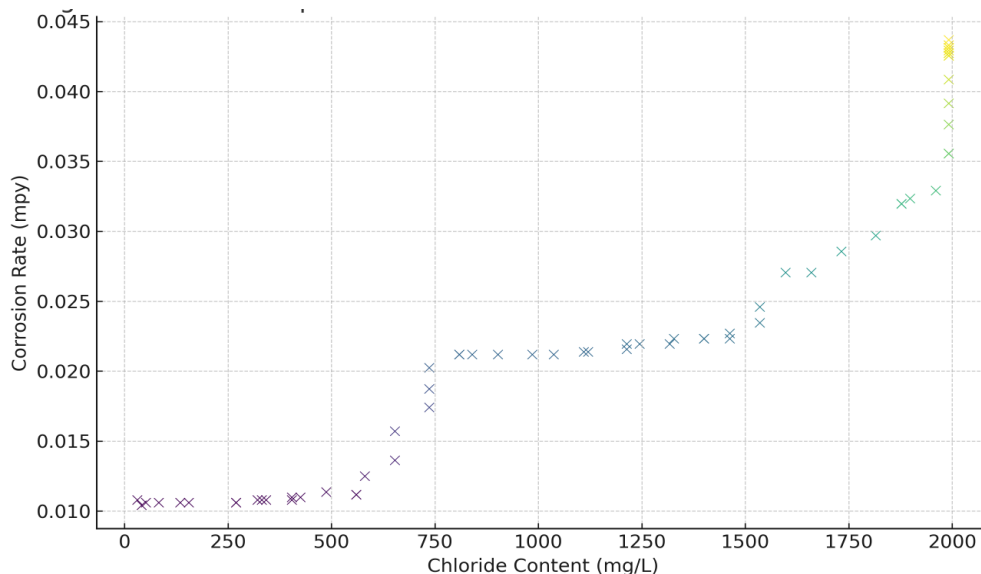


Figure 8. Scatter plot showing the relationship between the chloride content (mg/L) and the corrosion rate (mpy) of SS316L in a simulated cooling water environment. A clear upward trend demonstrates increased corrosion at higher chloride concentrations

Table 4. Comparison of the present study with representative literature on chloride-driven corrosion of 316L and related stainless steels

| Sl. No | Ref.                     | Material | Medium/ Application  | Exposure mode                             | Variables studied                                | Key reported finding   | What Present study adds beyond this  |
|--------|--------------------------|----------|--|---|--|--|--|
| 1      | (Malik et al., 1992)[54] | 316L     | Aqueous chloride solutions   | Static immersion/electrochemistry         | pH, [Cl <sup>-</sup> ], DO, temperature          | Pitting/corrosion behaviour strongly depends on chloride, pH, DO, temperature and flow; chloride increases susceptibility    | Replicate cooling-water operational features via cyclic exposure and isolate chloride/hardness effects rather than generic parameter scans                             |
| 2      | (He et al., 2009)[72]    | 316L     | Simulated formation water  | Static electrochemical + surface analysis | [Cl <sup>-</sup> ] with H <sub>2</sub> S synergy | High chloride affects oxide film semiconducting properties and dissolution; synergistic aggression with sulfide environments | Current environment is closer to reclaimed cooling water (neutral pH, cyclic temperature), and you introduce hardness as a mitigation lever under controlled chemistry |
| 3      | (Wang et al., 2019)[73]  | 316L     | Passivating electrolyte + chloride   | Electrochem + surface analytics           | Cl <sup>-</sup> in passivation conditions        | Chlorides alter passive state; film chemistry and structure change even before visible breakdown                             | To translate film-instability concepts into an operational threshold framework under cyclic cooling-water exposure and quantify corrosion rate consequences            |
| 4      | (Sun et al., 2024)[74]   | 316L     | Aggressive environment with Cl <sup>-</sup> -CO <sub>2</sub> -O <sub>2</sub> | Electrochemical + microscopy              | Cl <sup>-</sup> with gas chemistry               | Cl <sup>-</sup> compromises passive film and reduces corrosion resistance; combined environment shifts kinetics              | Present study holds other chemistry fixed and isolates chloride as primary stressor, then shows mitigation via hardness under cyclic cooling-water conditions          |

|   |                             |             |   |  |   |  |   |
|---|-----------------------------|-------------|---|--|---|--|---|
| 5 | Yoo et al., 2023 (PMC)[75]  | Type 316 SS | Groundwater-like conditions (waste containment) | Electrochem + modelling (RSM)          | Cl <sup>-</sup> , pH, HS <sup>-</sup>             | Establishes relationships between environmental factors and passive film breakdown/protection potentials | To provide a cooling-system relevant cyclic exposure framework and add hardness-mediated mitigation trends tied to corrosion rate (not only breakdown potentials)                   |
| 6 | (Coelho et al., 2025)[76]   | 316L        | Chloride media                                  | Potentiodynamic polarisation analytics | Pitting pathway identification                    | Shows distinct stable pitting growth pathways post-passivity breakdown                                   | Contribution is not pitting-pathway classification; it is the threshold + mitigation outcome under controlled cooling-water chemistry, with electrochemist + gravimetric validation |
| 7 | (Maatalah et al., 2024)[77] | 316L        | Simulated cooling water                         | Electrochemical                        | pH effects (and cooling-water relevant chemistry) | Cooling-water chemistry significantly alters corrosion behaviour and passivity stability                 | Present study extends cooling-water relevance by adding cyclic temperature exposure and explicitly mapping the chloride threshold region, plus hardness moderation                  |
| 8 | Present study               | 316L        | Simulated reclaimed cooling water               | Cyclic temperature + flow              | Cl <sup>-</sup> isolated + hardness               | threshold behaviour + hardness mitigation + cross-validation   | Addresses cyclic representativeness + combined chemistry  |

### 3.13.. Comparison with Prior Studies

Previous studies have determined that chloride ions leave passive films on austenitic stainless steels unstable and may cause localised corrosion at a certain critical chloride activity. The majority of studies, however, have been done in either a static immersion, constant temperature or with the limited consideration of the co-occurring ions that are characteristic of an industrial cooling water. Conversely, the current research incorporates cyclic exposure environments and quantifies the changes in chloride-controlled corrosion kinetics by hardness ions. Table 4 presents a summary of the representative literature and indicates the unique scope of the current work. This sorting out explains that the scientific enhancement in this case is not the overall point that chloride enhances corrosion, but the quantitative determination of a threshold-type reaction in a cyclical setting and the proof of hardness-mediated attenuation in a regulated, industrially significant water-chemistry model.

## 4. CONCLUSION

The present paper sheds light on the corrosion behaviour of Stainless Steel 316 L (SS316L) in chloride-saturated conditions that are specifically used to simulate the study conditions of reclaimed-water in industrial recirculating cooling systems. The results of our research prove that chloride-ion levels rise and have a positive correlation with SS316L corrosion, especially when localised corrosion-induced processes - pitting and crevice attacks - are accelerated, promoting material

degradation. It was observed that corrosion behaviour changed considerably beyond about 1000 mg/L. Passage of this limit resulted in the destabilisation of the chromium-enriched passive film, which resulted in the rapid localised corrosion, which was primarily in the form of pitting and crevice attack. From an industrial perspective, these findings have direct implications for material selection, water-chemistry management, and maintenance planning in reclaimed-water-based cooling systems.

Even though SS316L is capable of withstanding corrosion at reduced chloride concentrations (less than 500 mg/L), the passive protective layer breaks down significantly above a critical threshold (approximately 1000 mg/L). The moderating effect of water hardness is evident, and this is the area where corrosion literature fails to take this factor into account. High concentrations of calcium and magnesium are seen to improve the stability of the passive film, which has great potential as a way of corrosion mitigation without requiring the expensive replacement of materials.

The strength of this study lies in its ability to replicate key operational features of industrial cooling systems, including cyclic temperature variation, controlled ionic composition, and combined electrochemical-gravimetric assessment. This study is strong because it attempts to recreate real operating conditions through the application of cyclic temperature variations, controlled ionic conditions and a comprehensive array of testing

strategies which involve electrochemical analysis as well as gravimetric validation. These facts support the idea that the water chemistry in industries needs to be carefully optimised. Sustainability-related programs, including the use of reclaimed-water, indicate the importance of balancing the engineered foresight to avoid the system ineffectiveness and unintended degradation of materials.

#### 4.1. Limitations

Even though the methodology used in this study is rather sound, it has a number of limitations that should be taken into consideration. First, the experiments were carried out in a laboratory environment designed to model industrial cooling, but in real-life systems, things are much more complicated. The biofouling, varying pH levels, intermittent flow rates and mixed-metal assemblies were not recreated. In practice, these aspects can affect the corrosion behaviour. The pH of the water was kept at about 7.5, and the dissolved oxygen concentration was kept between 8 mg/L during the period of testing. The dynamics of corrosion of SS316L can change under such conditions, and these parameters may differ significantly in the real-world situation in an industry. Third, the exposure of cyclic testing was restricted to 14 days. It is an effective way of getting an immediate picture of short-term corrosion trends, but the future degradation process and cause of failures that commonly occur within the operating environment cannot be exhaustively covered. This study did not take into account microbiologically affected corrosion (MIC), even though it is relevant in the reclaimed water system and accelerates the process of corrosion. The experiment was based on SS316L. This alloy is popular, but the results are therefore not generalizable to other alloys or to other grades of stainless steel.

#### 4.2. Future Directions

In order to generalise the findings of the current study, the future study should address the gap between the laboratory simulation and the application in real life. Important experiments have been performed on SS316L in real conditions on cooling water in field operations, thus providing a complete picture of corrosion in a dynamic operational cycle (change of temperature), flow changes and intermittent chemical injection. Additional studies that should be pursued by future researchers include biochemical interactions, especially how microbial action triggers corrosion. Understanding of the interaction between microbiologically controlled corrosion (MIC), chloride ions and water hardness would significantly increase the applicability of the studies in reclaimed water conditions.

Another urgent area of concern is the study of galvanic interactions by considering multi-metal systems, as SS316L often exists in a combination with other metals in a complex assembly, e.g. a heat exchanger or a pipeline. The procedures that provide the guidelines that need to be followed in compatibility of the materials must be optimised when the interactions are being assessed, avoiding corrosion that is accelerated due to the dissimilarity of the metals.

In addition, in case the industries implement smart corrosion monitoring devices, which use real-time sensors and Internet of Things (IoT)-based data collection, they can change the way corrosion risks are managed and predicted. These technologies allow detecting in time, managing the lifecycle, and scheduling maintenance based on data. These systems should be tested alongside other inhibitors to consider a combination of them to improve performance, especially since sodium molybdate has shown promising results in the current study. The concept of sustainable implementation is dependent on the evaluation of the inhibitors, such as the long-term environmental effects. Lastly, more sophisticated water-chemistry models, taking into consideration chloride concentration, water hardness, temperature, flow dynamics, etc., will be developed to assist the predictive maintenance and guide the design of systems that are less prone to corrosion and maintenance needs. With these strategic directions, the industrial infrastructure will be more sustainable and environmentally aware.

#### Acknowledgement

*The authors acknowledge in a grateful manner that the Department of Civil Engineering, School of Engineering and Technology, Noida International University, was of great help in this research by facilitating the laboratory facilities and the technical assistance. The laboratory staff is also given a special thanks as they cooperated in installing the corrosion test rigs and kept the water chemistry parameters. The authors are thankful for the positive suggestions made by the peer reviewers, which were able to enhance the quality and clarity of this work.*

#### Authors' Contributions

Dr. Pradyut Anand conceptualised the study, designed the experiments, and supervised the project. Dr. Nitin Lamba was responsible for the electrochemical testing and data acquisition. Dr. Mohit Aggarwal performed gravimetric and chemical analyses and contributed to the literature review and result interpretation. All authors contributed to drafting and reviewing the manuscript and approved the final version for submission.

### Competing Interests

The authors declare that there are no competing interests related to the publication of this manuscript.

### 5. REFERENCES

- [1] T.Asano,R.Mujeriego, J.D. Parker (1988) Evaluation of Industrial Cooling Systems Using Reclaimed Municipal Wastewater. *Water Science & Technology*, 20(10), 163. <https://doi.org/10.2166/wst.1988.0134>
- [2] H.Kyllönen, J. Heikkinen, J.Ceras, J.Fernandez, O.Porc, O., A.Grönroos (2021) Membrane-based conceptual design of reuse water production from candy factory wastewater. *Water Science & Technology*, 84(6), 1389. <https://doi.org/10.2166/wst.2021.326>
- [3] J.Yang,M.Monnot, L.Ercolei, P. Moulin (2020) Membrane-Based Processes Used in Municipal Wastewater Treatment for Water Reuse: State-Of-The-Art and Performance Analysis [Review of Membrane-Based Processes Used in Municipal Wastewater Treatment for Water Reuse: State-Of-The-Art and Performance Analysis]. *Membranes*, 10(6), 131. Multidisciplinary Digital Publishing Institute. <https://doi.org/10.3390/membranes10060131>
- [4] M. Ali, M. A. Shams, N. Bheel, A. H. Almaliki, A. S. Mahmoud, Y. A. Dodo, O. Benjeddou, (2024) A review on chloride induced corrosion in reinforced concrete structures: lab and in situ. *RSC Advances*, 14(50), 37252. Royal Society of Chemistry. <https://doi.org/10.1039/d4ra05506c>
- [5] L. Awerbuch, M. Daye. (1994) Durability of concrete structures in the hostile service environment of desalination plants. *Desalination*, 97, 221. [https://doi.org/10.1016/0011-9164\(94\)00089-1](https://doi.org/10.1016/0011-9164(94)00089-1)
- [6] L. Bertolini, M. Gastaldi, (2010) Corrosion resistance of low-nickel duplex stainless steel rebars. *Materials and Corrosion*, 62(2), 120. <https://doi.org/10.1002/maco.201005774>
- [7] Z. F. Omar, D. Kurniawan, (2020) Effect of water treatment on AISI 316L stainless steel biocorrosion resistance. *AIP Conference Proceedings*, 2262, 40020. <https://doi.org/10.1063/5.0015826>
- [8] G. Meng, Y. Li, Y. Shao, T. Zhang, Y. Wang,F. Wang (2013) Effect of Cl<sup>-</sup> on the Properties of the Passive Films Formed on 316L Stainless Steel in Acidic Solution. *Journal of Material Science and Technology*, 30(3), 253. <https://doi.org/10.1016/j.jmst.2013.07.010>
- [9] Y. Yang, T. Lin, G. Wang, Y. Wang, M. Shao, F. Meng,F. Wang (2024) Corrosion Behaviors of Weathering Steels in the Actual Marine Atmospheric Zone and Immersion Zone. *Metals*, 14(8), 903. <https://doi.org/10.3390/met14080903>
- [10] A. Al-Gailani, O. Sanni, T. Charpentier, R. Crisp, J. H. Bruins, A. Neville (2020) Examining the effect of ionic constituents on crystallisation fouling on heat transfer surfaces. *International Journal of Heat and Mass Transfer*, 160, 120180. <https://doi.org/10.1016/j.ijheatmasstransfer.2020.120180>
- [11] S. Nolan, M. Rossini, C. Knight,A. Nanni (2021) New directions for reinforced concrete coastal structures. *Journal of Infrastructure Preservation and Resilience*, 2(1). <https://doi.org/10.1186/s43065-021-00015-4>
- [12] Md. S. Islam, K. Otani, M. Sakairi (2018) Corrosion inhibition effects of metal cations on SUS304 in 0.5 M Cl<sup>-</sup> aqueous solution. <https://www.sciencedirect.com/science/article/pii/S0010938X18300982>
- [13] A. D. Santos, E. Pinho, P. M. Reis, R. C. Martins, M. Gmurek, A. Nogueira, S. Castro-Silva, L. M. Castro,R. M. Quinta-Ferreira (2023) Heterogeneous photosensitization for water reuse in cellars: evaluation of silica, spongin, and chitosan as carrier material. *Environmental Science and Pollution Research*. <https://doi.org/10.1007/s11356-023-31178-0>
- [14] I. Tpyc, M. Gomelya, M. Киба, T. Pylypenko, T. Krysenko(2021) Development of Resource-Saving Technologies in the Use of Sedimentation Inhibitors for Reverse Osmosis Installations. *Journal of Ecological Engineering*, 23(1), 206. <https://doi.org/10.12911/22998993/144075>
- [15] N. Azzeri, F. Mancina, A. Tamba (1982) Electrochemical prediction of corrosion behaviour of stainless steels in chloride-containing water. *Corrosion Science*, 22(7), 675. [https://doi.org/10.1016/0010-938x\(82\)90047-6](https://doi.org/10.1016/0010-938x(82)90047-6)
- [16] J. E. Truman(1977) The influence of chloride content, pH and temperature of test solution on the occurrence of stress corrosion cracking with austenitic stainless steel. *Corrosion Science*, 17(9), 737. [https://doi.org/10.1016/0010-938x\(77\)90069-5](https://doi.org/10.1016/0010-938x(77)90069-5)
- [17] W. Faes, S. Lecompte, Z. Y. Ahmed, J. V. Bael, R. Salenbien, K. Verbeken,M. D. Paepe (2019) Corrosion and corrosion prevention in heat exchangers. *Corrosion Reviews*, 37(2), 131. <https://doi.org/10.1515/corrrev-2018-0054>
- [18] F. Lampert (2017) Thin Glass Coatings for the Corrosion Protection of Metals. *Research Portal Denmark*, 218. <https://local.forskningsportal.dk/local/dki-cgi/ws/cris-link?src=dtu&id=dtu-ff83a747-2076-4a11-8807-1eb064dcf49d&ti=Thin%20Glass%20Coatings%20for%20the%20Corrosion%20Protection%20of%20Metals>
- [19] M. N. Maria, W. M. K. W. M. Ikhmal, M. Amirah, S. A. Manja, M. S. Shaifudin, C. K. Sheng, M. F. M. Sabri, A. Adnan (2019) Green approach in anti-corrosion coating by using *Andrographis paniculata* leaves extract as additives of stainless steel 316L in seawater. *International Journal of Corrosion and Scale Inhibition*, 8(3). <https://doi.org/10.17675/2305-6894-2019-8-3-13>
- [20] B.Sarac, E.Sharifikolouei, Y.Zheng, E.Yüce, A. Asci, J. Keckes, A. S. Saraç,J. Eckert (2023) Enhanced Electrochemical and Corrosion Behavior of Amorphous 316-type Stainless Steel Microfibers in Saline Environment. *Research Square (Research Square)*. <https://doi.org/10.21203/rs.3.rs-2443500/v1>
- [21] R. S. Brito, M. do C. Almeida, N. C. B. Silva, S. Barreto, F. A. Dos R. Veríssimo (2021) Assessing intermittent saline inflows in urban water systems. *Water Science & Technology*, 85(1), 90. <https://doi.org/10.2166/wst.2021.622>
- [22] R. D. F. S. Costa, M. L. S. Barbosa, F. J. G. Silva, S. R. Sousa, V. F. C. Sousa, B. O. Ferreira (2023) Study of the Chlorine Influence on the Corrosion of

- Three Steels to Be Used in Water Treatment Municipal Facilities. *Materials*, 16(6), 2514. <https://doi.org/10.3390/ma16062514>
- [23] A. M. Anshar, B. Musa, M. Ayaz, S. Kasim, I. Raya, A. A. Ramírez-Coronel, S. Chowdhury, R. S. Zabibah, R. M. Romero-Parra, L. A. B. Arenas, Y. F. Mustafa, A. H. D. Al-Khafaji (2023) A Critical Review on Corrosion and Fouling of Water in Water Distribution Networks and Their Control. *Acta Chimica Slovenica*, 70(2), 173. Slovenian Chemical Society. <https://doi.org/10.17344/acs.2022.7939>
- [24] B. Bakshi, E. M. Doucette, S. Kyser (2021) Centralized softening as a solution to chloride pollution: An empirical analysis based on Minnesota cities. *PLoS ONE*, 16(2). <https://doi.org/10.1371/journal.pone.0246688>
- [25] T. E. Larson, R. V. Skold (1958) Laboratory Studies Relating Mineral Quality of Water To Corrosion of Steel and Cast Iron. *CORROSION*, 14(6), 43. <https://doi.org/10.5006/0010-9312-14.6.43>
- [26] N. Nelson, A. D. Luca (2021) Remineralization and Stabilization of Desalinated Water. In *IntechOpen eBooks*. IntechOpen. <https://doi.org/10.5772/intechopen.99458>
- [27] P. W. King, S. Peldszus, A. Mishra, B. F. Trueman, K. Aghasadeghi, G. A. Gagnon, D. E. Giammar, P. M. Huck (2022) Role of natural organic matter and hardness on lead release from galvanic corrosion. *Environmental Science Water Research & Technology*, 8(8), 1687. <https://doi.org/10.1039/d1ew00903f>
- [28] F. Presuel-Moreno, M. A. Jakab, N. R. Tailleart, M. Goldman, J. R. Scully (2008) Corrosion-resistant metallic coatings. *Materials Today*, 11(10), 14. [https://doi.org/10.1016/s1369-7021\(08\)70203-7](https://doi.org/10.1016/s1369-7021(08)70203-7)
- [29] S. Kiamehr (2014) Material Solutions to Mitigate the Alkali Chloride-Induced High Temperature Corrosion. *Research Portal Denmark*, 250. <https://local.forskningportal.dk/local/dki/cgi/ws/cris-link?src=dtu&id=dtu-51a869ee-f15d-4a7c-abea-5b2ec8246ac9&ti=Material%20Solutions%20to%20Mitigate%20the%20Alkali%20Chloride-Induced%20High%20Temperature%20Corrosion>
- [30] G. Kirby (1995) Fight chloride corrosion in aqueous systems. *Chemical Engineering Progress*, 91(2), 47. <http://www.osti.gov/scitech/biblio/6567684-fight-chloride-corrosion-aqueous-systems>
- [31] H. Pancheva, G. Reznichenko, N. Miroshnichenko, A. Sincheskul, A. Pilipenko, V. Loboichenko (2017) Study into the influence of concentration of ions of chlorine and temperature of circulating water on the corrosion stability of carbon steel and cast iron. *Eastern-European Journal of Enterprise Technologies*, 4, 59. <https://doi.org/10.15587/1729-4061.2017.108908>
- [32] M. Aliofkhaezai (2014) Developments in Corrosion Protection. In *InTech eBooks*. <https://doi.org/10.5772/57010>
- [33] S. Tsouli, A. Lekatou, E. Siozos, S. Kleftakis (2018) Accelerated corrosion performance of AISI 316L stainless steel concrete reinforcement used in restoration works of ancient monuments. *MATEC Web of Conferences*, 188, 3003. <https://doi.org/10.1051/mateconf/201818803003>
- [34] M. Wang, S. Zeng, H. Zhang, Z. Ming, C. Lei, B. Li (2020) Corrosion behaviors of 316 stainless steel and Inconel 625 alloy in chloride molten salts for solar energy storage. *High Temperature Materials and Processes*, 39(1), 340. <https://doi.org/10.1515/htmp-2020-0077>
- [35] H. Parangusan, J. Bhadra, N. Al-Thani (2021) A review of passivity breakdown on metal surfaces: influence of chloride- and sulfide-ion concentrations, temperature, and pH. *Emergent Materials*, 4(5), 1187. Springer Science+Business Media. <https://doi.org/10.1007/s42247-021-00194-6>
- [36] B. Zhang, J. Wang, B. Wu, X. Guo, Y. Wang, D. Chen, Y. Zhang, K. Du, E. E. Oguzie, X. Ma (2018) Unmasking chloride attack on the passive film of metals. *Nature Communications*, 9(1), 2559. <https://doi.org/10.1038/s41467-018-04942-x>
- [37] J. I. Ahuir-Torres, A. Al-Mahdy, M. Sharp, T. T. Opoz, G. Zhu, M. Bashir, H. R. Kotadia (2025) The influence of texture density and free surface energy on the corrosion resistance of laser-textured 316L stainless steel. *Npj Materials Degradation*, 9(1), xxx. <https://doi.org/10.1038/s41529-025-00622-6>
- [38] D. Grell, Y. Wilkin, P. F. Gostin, A. Gebert, E. Kerscher (2017) Corrosion Fatigue Studies on a Bulk Glassy Zr-Based Alloy under Three-Point Bending. *Frontiers in Materials*, 3. <https://doi.org/10.3389/fmats.2016.00060>
- [39] D. Torres, V. Vangrunderbeek, M. Bernal, G. M. Paldino, G. Bontempi, J. Ustarroz, L. B. Coelho (2023) Estimating pitting descriptors of 316L stainless steel by machine learning and statistical analysis. *Research Square (Research Square)*. <https://doi.org/10.21203/rs.3.rs-2921959/v1>
- [40] R. Clark, J. Searle, T. Martin, W. S. Walters, G. Williams (2019) The role of niobium carbides in the localised corrosion initiation of 20Cr-25Ni-Nb advanced gas-cooled reactor fuel cladding. *Corrosion Science*, 165, 108365. <https://doi.org/10.1016/j.corsci.2019.108365>
- [41] A. C. Stoot (2016) Protective coatings based on 2D-materials. *Research Portal Denmark*, 144. <https://local.forskningportal.dk/local/dki/cgi/ws/cris-link?src=dtu&id=dtu-e211260f-cf47-4684-a42f-1e031750b5d6&ti=Protective%20coatings%20base d%20on%202D-materials>
- [42] L. Zuo-Jia (2010) Effect of chloride ions on 316L stainless steel in cyclic cooling water. *Acta Metallurgica Sinica (English Letters)*, 23(6), 431. <https://doi.org/10.11890/1006-7191-106-431>
- [43] S. Kumar, R. Singh, N. S. Maurya (2023) Modelling of corrosion rate in the drinking water distribution network using Design Expert 13 software. *Environmental Science and Pollution Research*, 30(15), 45428. <https://doi.org/10.1007/s11356-023-25465-z>
- [44] T. Shabliy, Y. Nosachova, Y. Radovenchik, V. Vv (2017) Study of effectiveness of heavy metals ions as the inhibitors of steel corrosion. *Eastern-European Journal of Enterprise Technologies*, 4, 10. <https://doi.org/10.15587/1729-4061.2017.106974>
- [45] C. Chen, J. Zuo, Y. Wang (2020) An Electrochemical Investigation of Corrosion Behavior of 316L Austenitic Stainless Steel Reinforcement in Concrete Exposed to Acidic Environment.

- International Journal of Electrochemical Science, 15(2), 1634. <https://doi.org/10.20964/2020.02.48>
- [46] P. Li, Y. Wang (2022) Effect of chloride ions on the corrosion behavior of carbon steel in an iron bacteria system. *RSC Advances*, 12(24), 15158. <https://doi.org/10.1039/d2ra02410a>
- [47] H. An, G. Meng, Y. Wang, J. Wang, B. Liu, F. Wang (2020) Study on the Chloride Threshold and Risk Assessment of Rebar Corrosion in Simulated Concrete Pore Solutions under Applied Potential. *Coatings*, 10(5), 505. <https://doi.org/10.3390/coatings10050505>
- [48] H. E. H. BIRD, B. R. Pearson, P. A. Brook (1988) The breakdown of passive films on iron. *Corrosion Science*, 28(1), 81. [https://doi.org/10.1016/0010-938x\(88\)90009-1](https://doi.org/10.1016/0010-938x(88)90009-1)
- [49] F. Pessu, R. Barker, A. Neville (2020) CO<sub>2</sub> Corrosion of Carbon Steel: The Synergy of Chloride Ion Concentration and Temperature on Metal Penetration. *CORROSION*, 76(11). <https://doi.org/10.5006/3583>
- [50] A. N. Sánchez (2014) Forecasting Corrosion of Steel in Concrete Introducing Chloride Threshold Dependence on Steel Potential. Digital Commons - University of South Florida (University of South Florida). <https://scholarcommons.usf.edu/etd/5303>
- [51] J. Hesketh, E. J. F. Dickinson, M. L. Martín, G. Hinds, A. Turnbull (2021) Influence of H<sub>2</sub>S on the pitting corrosion of 316L stainless steel in oilfield brine. *Corrosion Science*, 182, 109265. <https://doi.org/10.1016/j.corsci.2021.109265>
- [52] L. Naixin, F. Anqing, H. Yu, G. Zhang, W. Chenghua, X. Wang, Z. Xu, Y. Wang (2025) Double effects of O<sub>2</sub> on passive film of super 13Cr stainless steel in CO<sub>2</sub> saturated environment. *Scientific Reports*, 15(1). <https://doi.org/10.1038/s41598-025-01208-7>
- [53] D. A. Lytle, M. Tang, A. T. Francis, A. J. O'Donnell, J. L. Newton (2020) The effect of chloride, sulfate and dissolved inorganic carbon on iron release from cast iron. *Water Research*, 183, 116037. <https://doi.org/10.1016/j.watres.2020.116037>
- [54] A. U. Malik, P. C. M. Kuty, N. A. Siddiqi, I. Andijani, S. Ahmed (1992) The influence of pH and chloride concentration on the corrosion behaviour of AISI 316L steel in aqueous solutions. *Corrosion Science*, 33(11), 1809. [https://doi.org/10.1016/0010-938x\(92\)90011-q](https://doi.org/10.1016/0010-938x(92)90011-q)
- [55] B. H. Oh, S. Y. Jang, Y. Shin (2003) Experimental investigation of the threshold chloride concentration for corrosion initiation in reinforced concrete structures. *Magazine of Concrete Research*, 55(2), 117. <https://doi.org/10.1680/mac.2003.55.2.117>
- [56] T. P. S. Gill, J. B. Gnanamoorthy, K. A. Padmanabhan (1987) Influence of Secondary Phases on the Localized Corrosion of Thermally Aged AISI 316L Stainless Steel Weld Metal. *CORROSION*, 43(4), 208. <https://doi.org/10.5006/1.3583138>
- [57] M. Y. Lu, R. Scipioni, B. Park, T. Yang, Y. Chart, S. A. Barnett (2019) Mechanisms of PrOx performance enhancement of oxygen electrodes for low and intermediate temperature solid oxide fuel cells. *Materials Today Energy*, 14, 100362. <https://doi.org/10.1016/j.mtener.2019.100362>
- [58] S. Banait, C. P. Paul, A. N. Jinoop, H. Kumar, R. Pawade, K. S. Bindra (2019) Experimental investigation on laser directed energy deposition of functionally graded layers of Ni-Cr-B-Si and SS316L. *Optics & Laser Technology*, 121, 105787. <https://doi.org/10.1016/j.optlastec.2019.105787>
- [59] P. Chakraborty, S. Neogy, N. K. Sarkar, H. Donthula, S. K. Ghosh, H. K. Nandi, B. Gopalakrishna, I. Balasundar, R. Tewari (2024) Formation of Bainite in a Low-Carbon Steel at Slow Cooling Rate – Experimental Observations and Thermodynamic Validation. *Steel Research International*. <https://doi.org/10.1002/srin.202400593>
- [60] R. Shi, Z. Wang, L. Qiao, X. Pang (2019) Microstructure evolution of in-situ nanoparticles and its comprehensive effect on high strength steel. *Journal of Material Science and Technology*, 35(9), 1940. <https://doi.org/10.1016/j.jmst.2019.05.009>
- [61] M. Bodunrin (2025) Corrosion Behaviour of S32101 (1.4162—X2CrMnNiN21-5-1) Stainless Steel in Pulping Liquors. <https://www.mdpi.com/1996-1944/18/9/1921>
- [62] X. Chen, H. Liu, X. Sun, B. Zan, M. Liang (2021) Chloride corrosion behavior on heating pipeline made by AISI 304 and 316 in reclaimed water. *RSC Advances*, 11(61), 38765. <https://doi.org/10.1039/d1ra06695a>
- [63] J. Alcántara, D. de la Fuente, B. Chico, J. Simancas, I. Díaz, M. Morcillo (2017) Marine Atmospheric Corrosion of Carbon Steel: A Review [Review of Marine Atmospheric Corrosion of Carbon Steel: A Review]. *Materials*, 10(4), 406. Multidisciplinary Digital Publishing Institute. <https://doi.org/10.3390/ma10040406>
- [64] P. Guo, E. C. L. Plante, B. Wang, X. Chen, M. Balonis, M. Bauchy, G. Sant (2018) Direct observation of pitting corrosion evolutions on carbon steel surfaces at the nano-to-micro- scales. *Scientific Reports*, 8(1). <https://doi.org/10.1038/s41598-018-26340-5>
- [65] B. Holmes, S. Bond (2007) Sour Service Limits of Dual-Certified 316/316L Steel. <https://www.twi-global.com/technical-knowledge/published-papers/sour-service-limits-of-dual-certified-316-316l-austenitic-stainless-steel-and-weldments-march-2010>
- [66] G. A. Gaber, L. Z. Mohamed, M. M. Tash (2020) Experimental correlation using ANOVA and DOE studies on corrosion behavior of Fe and Ni-based alloy under different media. *Materials Research Express*, 7(3), 36521. <https://doi.org/10.1088/2053-1591/ab7e6d>
- [67] B. Pradhan, B. Bhattacharjee (2008) Performance evaluation of rebar in chloride contaminated concrete by corrosion rate. *Construction and Building Materials*, 23(6), 2346. <https://doi.org/10.1016/j.conbuildmat.2008.11.003>
- [68] P. Li, Y. Wang (2011) Effect of Chloride on Corrosion Behavior of Reinforcing Steel HRB335. *Advanced Materials Research*, 1342. <https://doi.org/10.4028/www.scientific.net/amr.391-392.1342>
- [69] J.-W. Jang, I. Iwasaki (1991) Rebar Corrosion under Simulated Concrete Conditions Using Galvanic

- Current Measurements. CORROSION, 47(11), 875. <https://doi.org/10.5006/1.3585201>
- [70] K. Sipilä, M. Bojinov, W. Mayinger, T. Saario, M. Stanislawski (2015) Effect of chloride and sulfate additions on corrosion of low alloy steel in high-temperature water. *Electrochimica Acta*, 173, 757. <https://doi.org/10.1016/j.electacta.2015.05.137>
- [71] S. Akduman, H. Öztürk (2024) Effect of Reinforcement Corrosion on Structural Behaviour in Reinforced Concrete Structures According to Initiation and Propagation Periods. *Buildings*, 14(12), 4026. <https://doi.org/10.3390/buildings14124026>
- [72] W. He, O. Ø. Knudsen, S. Diplas (2009) Corrosion of stainless steel 316L in simulated formation water environment with CO<sub>2</sub>-H<sub>2</sub>S-Cl<sup>-</sup>. *Corrosion Science*, 51(12), 2811. <https://doi.org/10.1016/j.corsci.2009.08.010>
- [73] Z. Wang, A. Seyeux, S. Zanna, V. Maurice, P. Marcus (2019) Chloride-induced alterations of the passive film on 316L stainless steel and blocking effect of pre-passivation. *Electrochimica Acta*, 329, 135159. <https://doi.org/10.1016/j.electacta.2019.135159>
- [74] Q. Sun, F. Xie, Y. Zhang, D. Wang, M. Wu (2024) Stability of passive film and pitting susceptibility of 316 L stainless steel in the aggressive oilfield environment containing Cl<sup>-</sup>-CO<sub>2</sub>-O<sub>2</sub>. *Electrochimica Acta*, 499, 144709. <https://doi.org/10.1016/j.electacta.2024.144709>
- [75] J.-S. Yoo, N. T. Chung, Y. Lee, Y. W. Kim, J.-G. Kim (2023) Effect of Sulfide and Chloride Ions on Pitting Corrosion of Type 316 Austenitic Stainless Steel in Groundwater Conditions Using Response Surface Methodology. *Materials*, 17(1), 178. <https://doi.org/10.3390/ma17010178>
- [76] L. B. Coelho, T. Amand, D. Torres, M. Olivier, J. Ustarroz (2025) Identifying stable pitting pathways in 316 L stainless steel via fractal-inspired PCA-based clustering. *Npj Materials Degradation*, 9(1). <https://doi.org/10.1038/s41529-025-00594-7>
- [77] T. Maatallah, A. Houcine, F. Saeed, S. Khan, S. Ali (2024) Simulated Performance Analysis of a Hybrid Water-Cooled Photovoltaic/Parabolic Dish Concentrator Coupled with Conical Cavity Receiver. *Sustainability*, 16(2), 544. <https://doi.org/10.3390/su16020544>

## IZVOD

### KOROZIVNE PERFORMANSE SS 316L U OKRUŽENJIMA SA VISOKIM SADRŽAJEM HLORIDA: IMPLIKACIJE ZA INDUSTRIJSKE SISTEME ZA HLAĐENJE VODOM

*Rastuća upotreba recikliranih otpadnih voda u industrijskim recirkulacionim sistemima hlađenja dovela je do postepenog nakupljanja hlorida, što pokreće zabrinutost zbog dugoročnog ponašanja konstrukcionih materijala u korozivnom radu. Nerđajući čelik 316L (SS316L) se često koristi u ovim sistemima zbog svoje prirodne sposobnosti da se odupre koroziji, iako je pasivni sloj sklon raspadanju u prisustvu hlorida. Trenutna studija obuhvata istraživanje ponašanja SS316L u uslovima simuliranih cikličnih uslova rashladne vode, zajedno sa pažljivo kontrolisanom hemijom vode, sa posebnim fokusom na izolovanje uloge koncentracije hlorida i određivanje ublažavajućeg efekta tvrdoće vode. Elektrohemijski podaci i gravimetrijska analiza pokazale su da postoji jaka pozitivna korelacija između koncentracije hlorida i brzine korozije. Pri niskim nivoima hlorida (manje od 500 mg/L), SS316L je pokazao stabilnu pasivaciju sa niskim brzinama korozije (<0,015 mpy). Ipak, utvrđeno je da postoji kritična tačka od oko 1000 mg/L gde pasivni film nije mogao da se zadrži i lokalizovana korozija se ubrzala. Brzine korozije bile su veoma visoke na nivoima hlorida iznad 1500 mg/L, a u slučaju cikličnog izlaganja dostigle su 0,04 mpy. Uslov povećane tvrdoće vode, koju su predstavljali joni kalcijuma i magnezijuma, imao je značajan moderatorski efekat na koroziju izazvanu hloridima, jer je stabilizovao pasivni sloj i smanjio gustinu struje, posebno kada se koriste visoki nivoi hlorida. Ovi rezultati pokazuju da se optimizacija hemije vode, posebno kontrolisanom upotrebom koncentracije i tvrdoće hlorida, može koristiti kao isplativa i ekonomična mera za smanjenje korozije. Rezultati pružaju korisne informacije o tome kako povećati stabilnost materijala i operativnu konzistentnost industrijskih sistema za hlađenje koji rade koristeći recikliranu vodu.*

**ključne reči:** Korozija izazvana hloridom; nerđajući čelik 316L; ciklični sistemi za hlađenje vodom; tvrdoća vode; strategije za ublažavanje korozije.

*Naučni rad*

*Rad primljen: 20.01.2026.*

*Rad prihvaćen: 05.02.2026*

Pradyut Anand: 0000-0003-4055-2849

Nitin Lamba: 0000-0003-4510-1705

Mohit Aggarwal: 0000-0001-8993-6064